SEISMIC RESPONSE OF A SANDY STRATUM WITH A SILT LAYER UNDER STRONG GROUND MOTIONS

Bakhtiar Cahyandi Ridla[1), Huei-Tsyr Chen[2), M. Ruslin Anwar[3)

[1) Double Degree Program
E-mail: bakhtiar.ridla@gmail.com
[2) Department of Civil Engineering, National Central University
Jhongda Rd. 300 Jhongli City Taoyuan County Taiwan
[3) Department of Civil Engineering, University of Brawijaya
Jl. MT. Haryono 167 Malang, Indonesia;

ABSTRACT

The presence of silt layer with small permeability may exist in the liquefiable sandy ground and it can produce the water film beneath silt layer with high pore water pressure under earthquakes. From the geotechnical point of view, the water film can cause instability of ground especially for slope ground. The objectives of this study is to gain a more understanding the effect of possible crack inside the silt layer at certain time on the seismic responses of ground of liquefiable sand stratum with a silt layer through numerical simulations. A nonlinear 3D effective stress finite element program was used in this study. A total of 4 models were constructed. Two strong earthquakes with different characteristic were used in this study. Settlement on the surface and excessive pore water pressure were presented for all models. The result showed that possible crack in the silt layer can lead to the larger settlement due to the faster dissipation of EPWP beneath the silt layer and the breakage of silt layer can lead to the sudden decrease in EPWP in the soil beneath the silt layer and sudden increase in EPWP in the soil above the silt layer. Sometimes the upward movement of pore water may cause the soil to liquefy, which will not occur without the breakage of silt layer. The crack in the silt layer leads to the faster dissipation of EPWP below the silt layer; such faster dissipation progresses from the location beneath the silt layer to the bottom of the soil stratum.

Keywords: *liquefaction, numerical simulation, effective stress analysis, silt layer, crack*

INTRODUCTION

Liquefaction is a phenomenon in which the strength and stiffness of a soil are reduced by earthquake shaking or other rapid loading due to increase in excessive pore pressure. In this phenomenon, soil particles may deform with little shear resistance and then soil particles or grains behaving as a viscous liquid rather than as a solid can not support one another, inducing large deformation to cause damage to building and other structures as shown in the Figure 1. The damages induced by soil liquefaction are buildings' sinking into the ground or tilting, slope failures, nearly level ground to shift laterally tens of feet (lateral spreading), surface subsidence, ground cracking, and sand boiling.

Over the past years, many researchers have studied the liquefaction phenomenon which becomes one of the most important, interesting, and discussed topics in geotechnical earthquake engineering. To understand the mechanism of liquefaction, a majority of previous research have focused on homogenious sandy soil strata rather than non-homogenious soil strata.

The liquefaction phenomenon can easily occur in a uniform loose sandy soil stratum which has a tendency to compress when subjected to cyclic loading. However in the real field, the characteristic of soil is complicated. Silt layers with small permeability can exist in the sandy soil stratum. The existence of silt layer in a sandy soil stratum, especially for slope ground, can be very dangerous, this is because the small permeability of silt layer prevents the excessive pore water pressure from flowing upward during the earthquake shaking to develop a water film with high pore water pressure just beneath the silt layer, leading to failure of ground, especially the sloping ground, even long after the earthquake shaking. Such a phenomenon was seen in the 1964 Niigata earthquake where in Hakusan District, Niigata, a wide area started to move toward the Shinano River during the shaking and continued to move after the shaking ended; another one was seen in the 1987 New Zealand earthquake where lateral spread of the foundation ground put a bridge out of service for about one hour after the earthquake shaking ceased. These facts imply that a lateral spread or slope failure in a liquefied ground may not necessarily be caused by the inertia force of an earthquake, but by gravity force sustained after it due to the existence of a silt layer in the sandy ground where a water film develops at the bottom of the silt layer with high pores water pressure. (Kokusho, 1999).

In this study an effective-stress based three-dimensional finite element method will be used to numerically simulate the behaviour of liquefiable sandy soil stratum with a layer of silt. The objectives of this study is to investigate the effect of interval between P-wave and S-wave arrival, to clarify the effect of input motion, and possible crack in the silt layer on the seismic responses of ground of liquefiable soil sand stratum.

Mechanism of Liquefaction

In general, the actions in the soil which produce liquefaction phenomenon are as follows: seismic waves, primarily shear waves, passing through saturated granular layers, distort the granular structure, and cause loosely packed groups of particles to collapse while these collapses increase the pore-water pressure between the grains. If the pore-water pressure rises into a level approaching the weight of the overlying soil, the granular layer temporarily behaves as a viscous liquid rather than a solid, and then liquefaction has occurred.

(a)

(b)

Figure 1. Damage of Building and other structures caused by liquefaction: (a)Sand Boiling (b)Failure of abutment at Lyu Mei Bridge
(Provided from the investigation team for the 1999 Ji-Ji Earthquake by The Japanese Geotechnical Society)

Liquefaction Hazard

Some serious damages of the ground and building caused by liquefaction are flow failures, lateral spreading, ground oscillation, excessive settlement due to loss of bearing strength, sand boiling, tilting due to instability and overturning of structures. (1) *Flow Failure*. Flows develop in loose saturated sands or silts on relatively steep slopes, usually greater than 3 degrees. Figure 2 shows the diagram of a flow failure caused by liquefaction.

(2) *Lateral spreading*. Lateral spreading commonly disrupts foundations of buildings built on or across the failure mass, severe pipelines and other utilities in the failure mass, and compresses or buckles engineering structures, such as bridges, founded on the toe of the failure. Illustration of lateral spreading is shown in the figure 3 (3) *Ground Oscillation* (4) *Excessive Settlement*. Excessive settlement may be damaging, although they would tend to be much less than the large movements accompanying flow failures, lateral spreading, and bearing capacity failures. (5) *Sand Boiling*. This phenomenon is related to the excess pore water pressure to the ground surface caused by the pressures to the soil sand stratum during a loading such as an earthquake. In the liquefaction hazard, this phenomenon is also known as sand volcanoes. (6) *Tilting and Overturning of Structures.* When liquefaction occurs, the strength of the soil decreases and the ability of a soil deposit to support foundations for buildings and bridges are reduced as can be seen during a large earthquake.

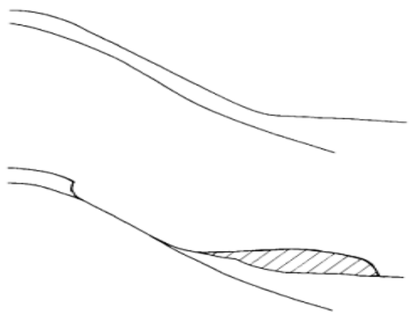

Figure 2. The diagram of a flow failure caused by liquefaction.
(Source: Youd,1992)

Susceptibility of Liquefaction

Reducing vulnerability and improving emergency response capabilities are two options to pursue in preparing for the possibility of liquefaction. With hazard zone maps, it is possible to identify areas with liquefiable potential and areas of minor and major concern. There are several ways to evaluate the liquefaction susceptibility of soil as shown below Kremer (1996): (1) *Historical Criteria* (2) *Geological Criteria* (3) *Compositional Criteria* (4) *State Criteria.*

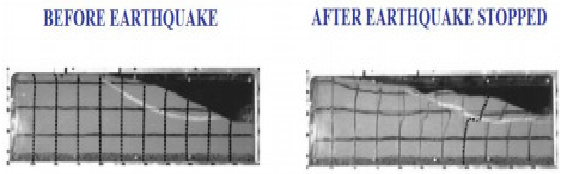

Liquefaction on non-uniform Soil Stratum (Intralayers of Silt Case)

Fellenius (2009) defined that a silt layer is a sedimentary material consisting of grains or particles of disintegrated rock, while the size is smaller than sand but larger than clay. He defined that the diameter of the silt particles ranges from 0.002 to 0.0006 mm in where this particle is often found at the bottom of bodies of water where it accumulates slowly by settling through the water. Based on this literature, the permeability of silt is lower than sand, while during the shaking and liquefaction the silt layer can produce the water film beneath silt layer.

The water film phenomenon is very dangerous for ground, especially for slope ground, because it can cause lateral spreading and slope failure for ground. Kokusho (1999) and Kokusho and Kojima (2002) investigated the effect of water film formed beneath relatively impervious sublayers in a liquefied sand layer by doing experiments using 1D and 2D models, and concluded that failure can be caused by the formation of a water film at the base of a sublayer leading to a zone of essentially zero strength.

Simatupang (2011) investigated the effect of existence of multiple layers of silt in the sandy soil stratum. He compared seismic response of a liquefiable sandy soil stratum between homogenious sand layer and non-homogenious layer (a layer of silt inside soil sand stratum). Based on his research, the existence of intra layers of silt in the sandy soil stratum can reduce the extent of liquefaction and it can significant reduce the ground settlement.

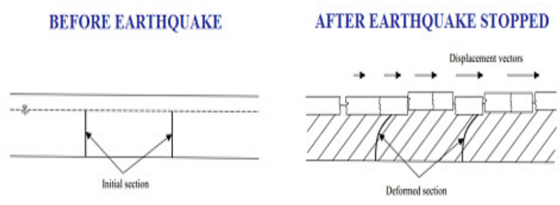

(a) (b)

Figure 3. The illustration of the lateral spreading involve lateral displacement of a subsurface layer: (a) No slope ground condition , (b) Gently sloping ground (Source: (a) Youd, 1992 (b) Malvick et.al, 2004)

In 1991, Kuttel and Fiegel explained the mechanism of liquefaction in the non-homogenous soil stratum by using a concept of water interlayer (water film) near the interface of soil layers with different permeability and described a mechanism applicable to liquefaction in layered or stratified soil deposits. In their research, they performed a centrifuge shaking table test to demonstrate the formation of water films in layered sand and concluded that the non- uniformity of the overlying impermeable bridges are reduced as can be seen during a large earthquake.

Phenomenon of Crack Layer in Liquefaction

Cracking phenomenon may occur at the thinnest section of the overlying layers. This phenomenon happened because bulging and high pressure gradients tend to weaken the overlying soil layer. Soil cracking can be dangerous for the stability of slopes because cracked zones are weaker and more permeable. In addition, the presence of cracks at certain layer induces significant changes on permeability, compressibility, and the strength of soil. Kuttel and Fiegel (1991) explained that cracking at certain layer can cause the volume of water to accumulate at the interface escapes at relatively high velocity and the erosion of both the overlying and liquefiable soils.

On the other hand, cracking phenomenon at the certain layer has an advantage to decrease the presence of water films on the propagation of pore water pressure at the time. As mentioned by Malvick, et.al. (2008), geologic heterogeneities, ground cracking and sand boil formation processes can be expected to affect both the thickness of the dilating zone and the consequences of water film formation. Crack layer at certain time on the propagation of earthquake motion is shown in the **Figure 4**.

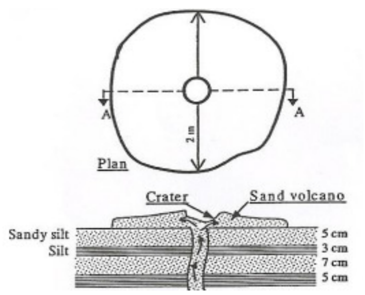

Figure 4. Cross section of crack layer at certain time on the propagation of earthquake motion
(Source: Byrne et. al, 2007)

METHODOLOGY

In performing the numerical simulation the three-dimensional nonlinear eff ective stress finite element method was adopted (Jou, 2000). This method is developed on the basis of Biot theory for porous media. The nonlinear soil behavior was modeled using the Cap model with Mohr-Coulomb type failure line and the pore pressure model consistent with the Cap model was adopted (Pacheco,1989). The lateral boundaries can be modeled as either roller-type boundaries or absorbing boundaries, while the bottom bedrock is always fixed.

This method adopts the U-W form of equation of motion (Zienkiewicz and Shiomi, 1984) as follows:

$$\begin{bmatrix} m_{uu} & m_{uw} \\ m_{uw}^T & m_{ww} \end{bmatrix}\begin{Bmatrix} \ddot{\bar{u}} \\ \ddot{\bar{w}} \end{Bmatrix} + \begin{bmatrix} c_{uu} & c_{uw} \\ c_{uw} & c_{ww} \end{bmatrix}\begin{Bmatrix} \dot{\bar{u}} \\ \dot{\bar{w}} \end{Bmatrix} + \begin{bmatrix} k_{uu} & k_{uw} \\ k_{uw}^T & k_{ww} \end{bmatrix}\begin{Bmatrix} \bar{u} \\ \bar{w} \end{Bmatrix} = -\begin{bmatrix} m_{uu} & m_{uw} \\ m_{uw}^T & m_{ww} \end{bmatrix}\{J\}\ddot{\phi}$$

where $\overline{u}$ is the displacement of soil particle and $\overline{W}$ is the displacement of water relative to soil particle. The vector {J} is made up of 1's and 0's to account for the desired direction of input motion $\ddot{\phi}$ is the input motion specified at the bedrock of soil stratum. It should be pointed out that in this study the excessive pore water pressure (EPWP) was computed at the center of element.

VERIFICATION AND VALIDATION

A good agreement can be seen in the previous study (Simatupang, 2011). The validity of the current program was verified by comparing with a centrifuge test result of a silt layer embedded in a liquefiable sandy ground (Lee et al., 2010).

In this study the validation and verification of numerical simulation was further made by comparing with the centrifuge test results for silty soils with and without 45 stone columns (Adalier et al., 2003). Both of models can be shown in **Figure 5** and **Figure 6**. The models used in centrifuge test can be seen in the **Figure 5**. The characteristic and the size of finite element model for numerical simulation can be seen in the **Figure 6**. The input motions was a 20-cycle harmonic base input motion of increasing amplitude with the maximum value being 0.3g and 1.8 Hz prototype frequency; the duration of motion is about 13 seconds as seen in the **Figure 7**. Settlement and excess pore water pressure were observed in this study. **Figure 8** compares the settlement on the surface. **Figure 9** compares the development of EPWP at several depths. A good agreement can be observed for both of comparisons.

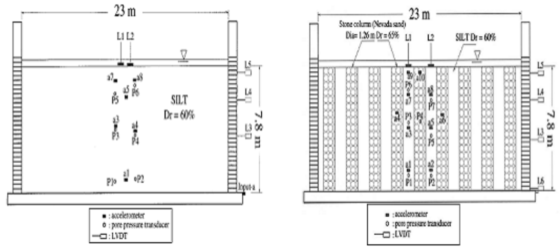

(a) (b)

Figure 5. Centrifuge Models: (a) Silty Model, and (b) Sand Stone Column Model (Source: (Adalier et al. ,2003)

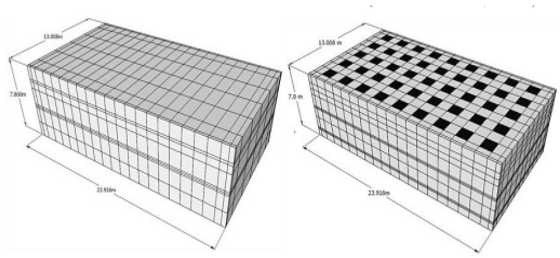

(a) (b)

Figure 6. Finite Element Models: (a) Silty Model, and (b) Sand Stone Column Model

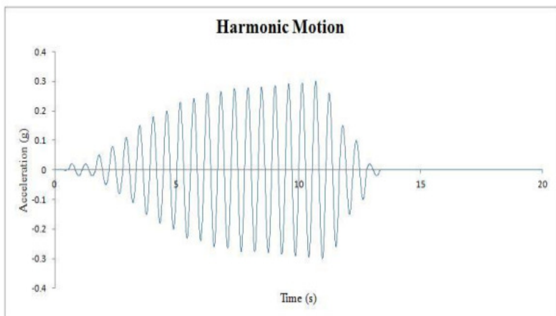

Figure 7. Finite Element Models: (a) Silty Model, and (b) Sand Stone Column Model

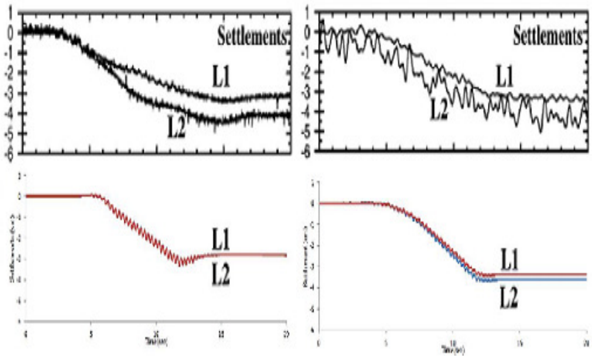

(a) (b)

Figure 8. Comparison of Settlement on the surface between Centrifuge Test Results (top) and Numerical Simulation (bottom) : (a) Silty Soils and (b) Silty soils with 45 stone columns.

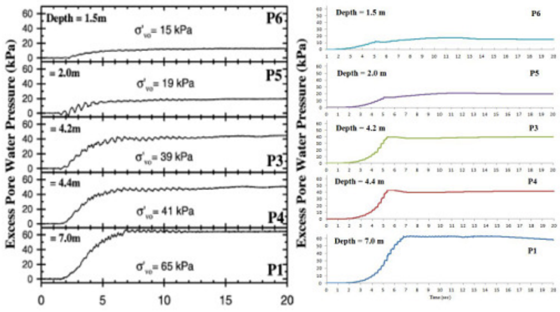

(a)

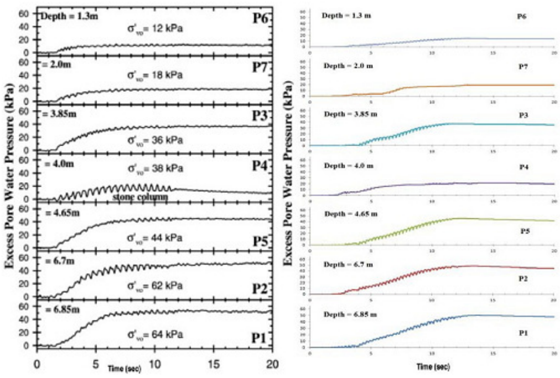

(b)

Figure 9. Comparison of excess pore water pressure between Centrifuge Test Results (left) and Numerical Simulation (right) : (a) Silty Soils and (b) Silty soils with 45 stone columns.

NUMERICAL RESULTS AND DISCUSSIONS

In the previous studies, it was found that the pore water pressure beneath silt layer will become higher due to the impermeable character of silt layer. This can be dangerous for instability of ground surface especially when it is happened in the slope ground, because due to slower dissipation, the water film produced during the motion will remain even after the motion stops, leading to slide or lateral movement of the ground. In the following analysis an attempt was made to see if the breakage of a silt layer can lead to the faster dissipation rate of EPWP of the soil beneath the silt layer.

Model Description

Shown in Fig. 10 is the finite element model adopted to investigate the effect of breakage of a silt layer on the EPWP. The size of model consists of 69.12 m x 42.64 m x 24 m. This model was divided into 13 layers with the top and bottom layer having the thickness of 1.2 m and the remaining layers with thickness of 2.4 m for each layer. The existence of silt layer can be found at the depth of 9.6 m from the surface in this model. In this study, only two cases were considered. Case 1 is the case where the silt layers remain intact during the analysis. Case 2 is the case where the silt layer was crack at 30 seconds after the motion started which is modeled by changing the permeability of silt layer to 10^{-4} m/sec. The area of crack is equivalent to 10 % at center area of silt.

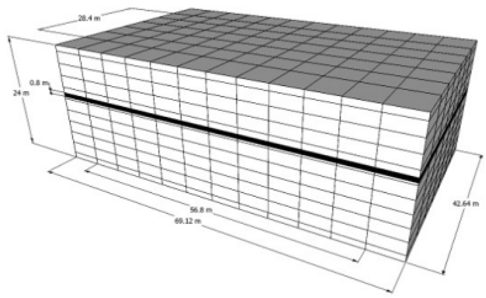

(a)

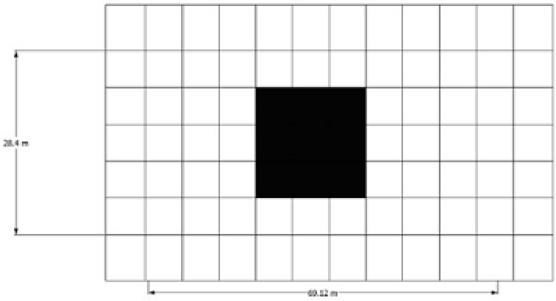

(b)

Figure 10. Finite Element Model for Investigating the Effect of Crack in Silt Layer: (a) Full View, (b) Cracked location.

The strong Chi-Chi earthquake motion in 1999 recorded in Chiayi station and Taipei station were used in this study. The figures of Chi-Chi earthquake in 1999 for both stations as mentioned above can be seen in the **Figure. 11**.

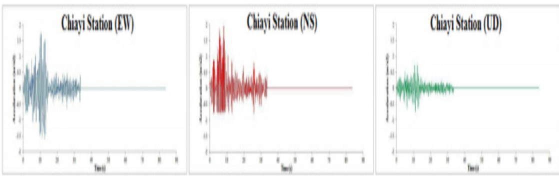

(a)

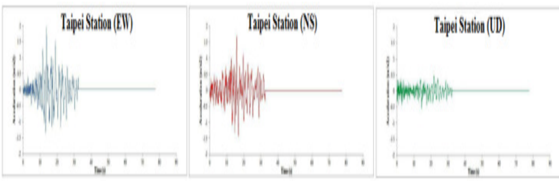

(b)

Figure 11. Three strong earthquakes with three components of direction: (a) Chiayi station (b) Taipei station

Results and Discussion

Figure 12 depicts the time histories of settlement for Case 1 and Case 2 subjected to Chiayi input and Taipei input. The settlement for both cases starts at 0.8 seconds and remains the same until 20 seconds and the settlement at 20 seconds for both cases is approximately 29.2 cm. Then at 20 seconds, some elements inside silt layer for case 2 crack due to high EPWP development below the silt layer. Within this cracked area, EPWP generated beneath the silt layer can easily move through the silt layer. The effect of the crack in the middle area of silt layer can be observed from the settlement after 20 seconds. After 20 seconds, the rate of increment in the settlement for case 2 will be larger than that of case 1 until the end of simulation. The maximum settlements at the end of simulation for Case 1 and Case 2 are approximately 68 cm and 77 cm, respectively. The larger settlement of the case 2 is due to the fact that the faster dissipation of EPWP leads to the increase in settlement. The similar trends in the time histories of settlement can also be seen for Taipei input.

Figure 13 shows time histories of EPWP ratios at the depths of 0.6 m, 4.8 m, 9 m, 10.6 m, 14.4 m, and 19.2 m for Case 1 and Case 2 subjected to Chiayi input. At the depth of 19.2 m, liquefaction does not occur for both cases. The same values of EPWP ratio can be seen at the beginning of motion until 20 seconds for both cases. Otherwise, at 20 seconds when the middle area of silt layer cracks for case 2, the difference can be seen between two cases. The EPWP ratios for Case 2 decrease slightly faster than those of Case 1 after 30 seconds until the end of simulation, although elements inside silt layer crack at 20 seconds.

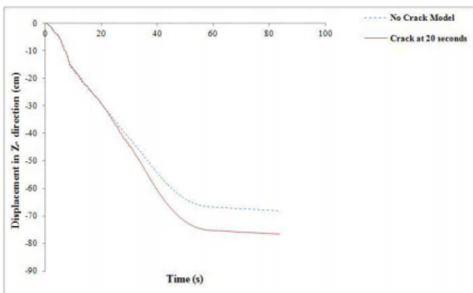

(a)

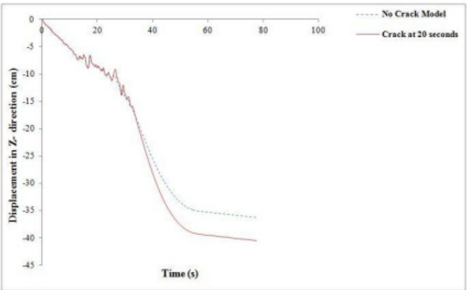

(b)

Figure 12.Time history of settlement on the surface for Case 1 and Case 2 subjected to: (a) Chiayi station (b) Taipei station

At the depth of 14.4 m, liquefaction occurs for both cases. In general, the trend in the time histories is similar to that at the depth of 19.2 m. However, the difference is larger after 20 seconds, as compared with that at the depth of 19.2 m. At the depth of 10.6 m, which is beneath the silt layer, liquefaction occurs for both cases. The trend is in general similar to that at the depth of 19.2 m and 14.4 m. However, because of the crack in the silt layer above it, a sudden decrease in EPWP ratio can be observed at 20 seconds, leading a larger difference between both cases as compared the case at the depth of 14.4 m. At the depth of 9 m, the liquefaction does not occur for Case 1. For Case 2 liquefaction does not occur until 20 seconds. However, a sudden increase in EPWP occurs at 20 seconds because of the crack in the middle area of silt layer cracked. Such an increase then causes the soil to liquefy.

At the depths of 4.8 m and 0.6 m, liquefaction occurs for both cases. Because of the dissipation of EPWP due to the crack in the silt layer, at both depths, the EPWP is larger for Case 2, leading to dissipation of EPWP of Case 2 being slower than that of Case 1. However, the difference after 20 seconds becomes smaller as depth decreases.

Shown in **Figure 14** are the initial effective stress and the EPWP profiles for Case 1 and Case 2 at several selected time. Both cases have the same value of EPWP up to 20 seconds before cracks occur in the silt layer. At 30 seconds, the crack in the silt layer leads to the faster dissipation of EPWP below the silt layer; such faster dissipation progresses from the location beneath the silt layer to the bottom of the soil stratum. On the other hand, because of the upward movement of pore water pressure, the EPWP becomes higher for Case 2 and slower dissipation for the soil above the silt layer. This phenomenon indicates that the breakage in the silt layer can lead to the faster dissipation of EPWP of the soil beneath the silt layer and may cause the soil above the silt layer to liquefy which will not occur without the breakage of silt layer.

Figure 15 depicts the time histories of EPWP ratio at the depths of 0.6 m, 4.8 m, 9 m, 10.6 m, 14.4 m, and 19.2 m for Case 1 and Case 2 subjected to Taipei input. Figure 16 shows the initial effective stress and the EPWP profiles for both cases at several selected times. In general, the trend is similar for all depths to that of Chiayi input. However, one can observe that the development of EPWP for Taipei input is slower than that for Chiayi input; it is due to the fact that the acceleration of Taipei input is smaller slower than Chiayi input in the early phase where Taipei input delays for about 7 seconds. In addition, the dissipation of EPWP for the case with Taipei input is faster than Chiayi input which starts after 32.5 seconds for Taipei input and 33.6 seconds for Chiayi input, respectively.

From the above discussions, it can concluded that in general, for the effect of crack in the silt layers, the trends in the time histories of EPWP ratio and profile are similar among Chiayi input and Taipei input and the duration of earthquake motions play important role in the evaluation the seismic response of soil stratum.

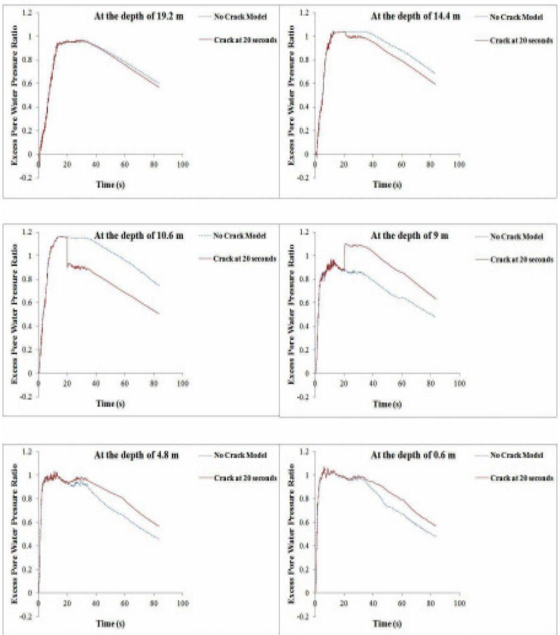

Figure 13. Time history of excess pore water pressure ratios at different depths for Case 1 and Case 2 subjected to Chiayi input.

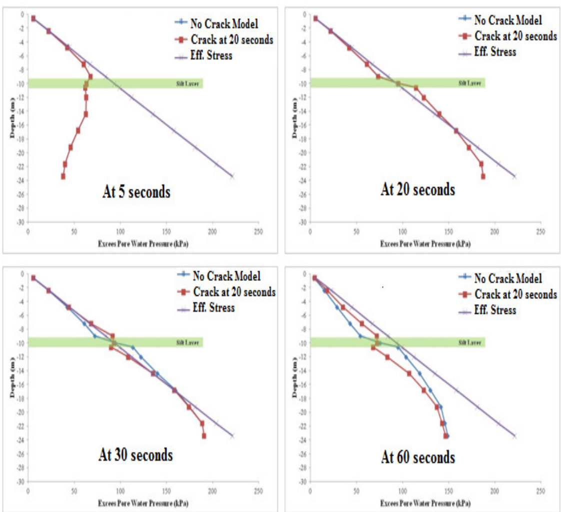

Figure 14 Initial effective stress and excess pore water pressure profile for Case 1 and Case 2 subjected to Chiayi input at several selected times.

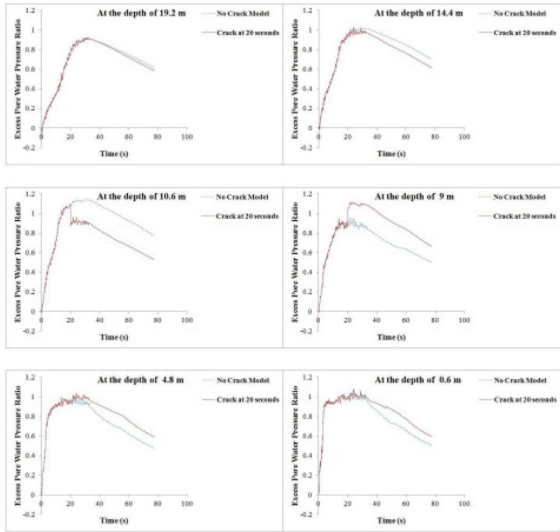

Figure 15. Time history of excess pore water pressure ratios at different depths for Case 1 and Case 2 subjected to Taipei input.

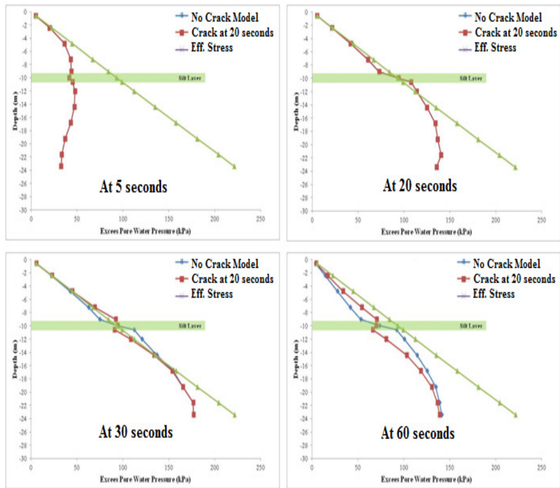

Figure 16. Initial effective stress and excess pore water pressure profile for Case 1 and Case 2 subjected to Taipei input at several selected times.

CONCLUSIONS AND RECOMMENDATIONS

Conclusion

a) The crack in the silt layer can lead to the larger settlement due to the faster dissipation of EPWP beneath the silt layer.

b) The crack in the silt layer leads to the faster dissipation of EPWP below the silt layer. Such a phenomenon may cause the soil above the silt layer to have the larger EPWP and that below the silt layer to have smaller EPWP.
c) Duration of earthquake affects the seismic responses of ground.

Recommendations

a) Further investigations on the soil sand stratum with inclined silt layer is needed to gain a better understanding of the effect of water film and the mechanism of lateral spreading on the liquefiable sandy soil stratum.
b) As for the continuation of crack study, the variation in time for the occurrence of crack and the size effect of crack area can be further investigated.

   By understanding this situation, a new method to reduce the liquefaction effect can be proposed in the future..

REFERENCE

Kokusho T. (1999), “Water Film in Liquefied Sand and Its Effect on Lateral Spread”, Journal of Geotechnical and Geoenvironmental Engineering, ASCE, Vol. 125, No.10, pp 817-826

Kokusho T., Kojima T. (2002), “Mechanism for Post-Liquefaction Water Film Generation in Layered Sand”, Journal of Geotechnical and Geoenvironmental Engineering, ASCE, Vol.128, No.2, pp. 129-137

Adalier K., Elgamal A-W., Meneses J., Baez J.I. (2003), “Stone Columns as Liquefaction Countermeasure in Non-Plastic Silty Soils”, Soil Dynamics and Earthquake Engineering, Vol. 23, No. 7, pp. 571-584

Nesgaard E., Byrne P.M. (2005), “Flow Liquefaction due to Mixing of Layered Deposits”,

Simatupang R. M., (2011), “ A Numerical Investigation on Stone Columns as a Countermeasure for Liquefaction of Sandy Soil Stratum With Intralayers of Silt”, Master Thesis, Department of Civil Engineering, National Central University, Chungli, Taiwan